Available online at www.sciencedirect.com
SCIENCE DIRECT®
Journal of Nuclear Materials 335 (2004) 359–365
journal of nuclear materials
www.elsevier.com/locate/jnucmat

Characterization of hydrogen concentration in Zircaloy claddings using a low-frequency acoustic microscope with a PVDF/LFB transducer

Che-Hua Yang *, Ming-Fong Huang

Department of Mechanical Engineering, Chang Gung University, 259 Wen-Hua 1st. Rd., Kwei-Shan, Taoyuan, Taiwan

Received 16 September 2003; accepted 18 July 2004

Abstract

Hydrogen embrittlement is one of the major mechanisms responsible for the degradation of ductility of Zircaloy cladding materials. Currently the characterization of hydrogen concentration (HC) very often relies on destructive methods that are time-consuming and costly. In this research, an ultrasound-based nondestructive evaluation (NDE) technique is reported for the determination of HC in Zircaloy claddings. This ultrasound-based NDE technique employs a low frequency acoustic microscope (AM) with a PVDF/LFB transducer and a Fourier-based signal processing technique. With this AM technique, a relation between the ultrasound wavespeed and the HC of Zircaloy is established. A resolution of HC measurements with the current technique is demonstrated to be better than 200 ppm. This NDE technique has been developed with an aim to have a better resolution and also to be potentially applied to pool-side inspection.

PACS: 28.41.Te

1. Introduction

Zircaloy cladding can undergo considerable changes in mechanical properties while in reactor service. It has been established that precipitated hydrides are responsible for hydrogen embrittlement of zirconium and alloys [1]. The degree of embrittlement was reported to be affected mainly by hydrogen concentration [2]. The hydriding phenomena have been studied on uptake mechanism [3,4], solubility [5], reduction of ductility [2,6–9] and the behavior in reactors [10].

The characterization of hydrogen concentration (HC) in Zircaloy cladding materials during the course of reactor service is an important task. Very often, the hydrogen concentration of Zircaloy fuel cladding is determined by off-line characterization techniques such as an inert-gas fusion, hot-vacuum extraction method [11], quantitative metallographic analysis for acid-etched samples and other destructive methods in laboratories. These techniques first suffer the drawbacks of transport operation and substantial sampling efforts of irradiated cladding materials, which are time-consuming and costly. Recently, works has been made to develop non-destructive techniques based on neutron radiography (NRG) techniques such as neutron imaging plate (IP) and computed tomography (CT) for estimation of HC

* Corresponding author. Fax: +886 03 328 3031.
E-mail address: yang@mail.cgu.edu.tw (C.-H. Yang).

0022-3115/$ - see front matter © 2004 Elsevier B.V. All rights reserved.
doi:10.1016/j.jnucmat.2004.07.045

in Zircaloy fuel cladding materials [12]. Regardless of the proven detection sensitivity, these NRG techniques rely on complicated and expensive equipment, which are difficult for poolside inspection applications.

Poolside nondestructive evaluation (NDE) technique is desired for the characterization of HC in fuel cladding materials. Eddy current technique has been attempted for the characterization of HC in Zircaloy fuel cladding materials, but proved no adequate resolution in the detection of HC [13]. Ultrasonic techniques have been reported to characterize nuclear fuel cladding materials [14,15]. In particular the ultrasonic technique, in which the ratio of longitudinal to shear wave velocity is used to correlate with HC in Zircaloy, is of technological interest [16].

In 1985, Kushibiki and Chubachi [17] developed a line-focus-beam (LFB) lens for a high-frequency (225 MHz) acoustic microscope (AM). The LFB lens enables an AM for a polarization-sensitive measurement of phase velocities of surface waves propagating in anisotropic materials. In 1996, Xiang et al. [18] developed a lens-less LFB transducer using a polyvinylidene fluoride (PVDF) film as a sensing element. The PVDF/LFB transducer is compatible with a pulser/receiver commonly used in NDE applications, but trading off the high spatial resolution which is not always necessary in material characterizations. The electromechanical coupling of PVDF film is lower than that of piezoceramic. However, the PVDF film has a greater damping and exhibits a broadband nature. Most important, the PVDF film is flexible and can be used to construct ultrasound transducers with variable sensing geometry.

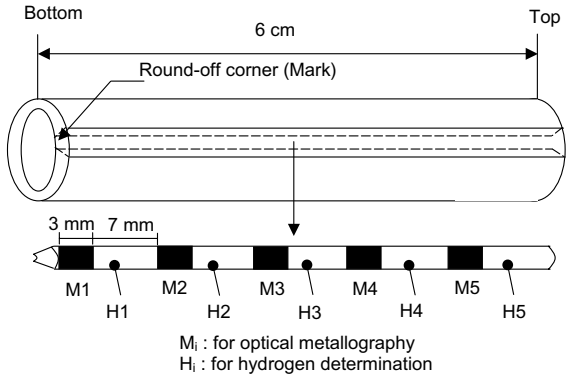

Fig. 1. A schematic showing typical geometry of Zircaloy claddings.

This research describes a low-frequency AM technique with a PVDF/LFB transducer for the characterization of HC in Zircaloy fuel claddings. Details of the cladding samples, measurement principle, equipment configuration, and measurement results are described in the following sections.

2. Zircaloy cladding samples and HC measurements

Zircaloy-4 cladding samples are prepared with the dimensions of 60 mm in length, 10.80 mm in outer

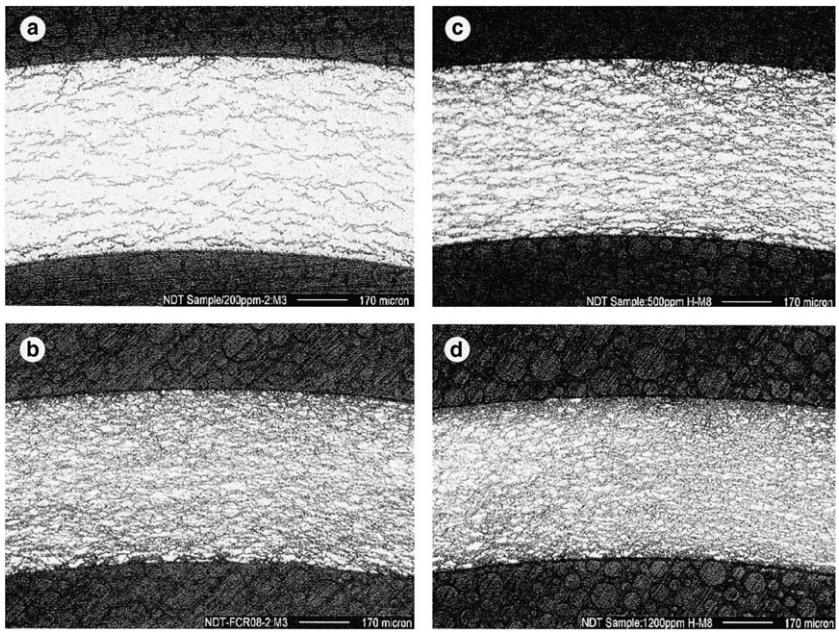

Fig. 2. Optical micrographs for the hydrogen-charged Zircaloy claddings: (a) FCR02; (b) FCR05; (c) FCR08 and (d) FCR12.

Table 1
A table showing the measured HCs for the five Zircaloy claddings

Sample	HC (ppm)						
	Axial site					Average	Standard deviation
	H1	H2	H3	H4	H5		
Archive	0						
FCR02	199	212	210	213	210	209	5
FCR05	462	423	416	399	441	428	22
FCR08	751	762	675	796	715	740	41
FCR12	1091	1143	1058	1136	920	1070	81

diameter, and 0.64 mm in wall thickness. Fig. 1 shows typical sample geometry. A slice of the Zircaloy tube is removed from the cladding. This slice is further partitioned into 10 parts, M1–M5 for optical metallography, and H1–H5 for hydrogen determination using a destructive method. The HCs of H1 through H5 are determined by an inert gas fusion method using LECO RH-404 hydrogen determinator (LECO Corp.). Five Zircaloy samples are tested. An archive Zircaloy specimen is prepared without hydrogen. The other four samples are hydrogen-charged to target bulk HCs of 200 ppm (labeled as FCR02), 500 ppm (FCR05), 800 ppm (FCR08) and 1200 ppm (FCR12) by weight. Fig. 2 shows typical micrographs (M3) for the four hydrogen-charged claddings, Fig. 2(a) for the FCR02 sample, 2(b) for FCR05, 2(c) for FCR08, and 2(d) for FCR12, respectively. The measured HCs for the hydrogen-charged cladding samples are listed in Table 1. Among the five samples, the measured HCs for the FCR02 sample have an average of 209 ppm with a standard deviation of 5 ppm. This result indicates that the FCR02 sample is hydrogen-charged uniformly closed to its targeted value of 200 ppm. However, for samples with higher bulk HCs, it is shown that the difference between the averaged and targeted HCs increases, and the standard deviation increases as well. The measured HCs for the FCR12 sample have an average of 1070 ppm, 130 ppm below the targeted value of 1200 ppm, and a relatively high standard deviation of 81 ppm is observed.

3. Measurement principle

The underlying principle of the current NDE technique is to detect the change of ultrasonic wavespeed caused by hydrogen in Zircaloy claddings. Hydrogen in Zircaloy claddings can cause a minor change in ultrasonic wavespeed, the phase velocity for example, due to the change of mechanical properties. However, the change of wavespeed caused by hydrogen is extremely small, and requires a measurement with high accuracy. On the other hand, ultrasonic waves propagating in the claddings are dispersive, meaning that the ultrasonic waves have wavespeeds depending on their frequencies.

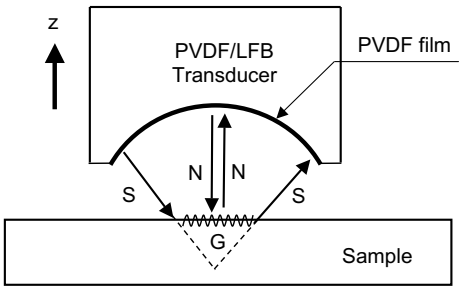

Fig. 3. A schematic showing the operational principle of a acoustic microscope (AM) used for material characterizations.

The operational principle based on a geometrical acoustics model for a quantitative AM is illustrated in Fig. 3. Two acoustic paths are important when the LFB transducer is used in measuring the phase velocity of ultrasonic waves propagating along claddings. The first acoustic path contains an acoustic ray generated by the transducer (labeled as downward N) and another acoustic ray directly reflected by the sample (upward N). In the second acoustic path, an oblique acoustic ray (S) generated by the transducer excites a guided wave (G) traveling along the sample, and radiates back to the transducer through the acoustic ray S. Acoustic waves propagating along N-rays and S-rays have a wavespeed of 1480 m/s as the ultrasound wavespeed of water at room temperature. The phase velocity of the guided wave (G) carries the information of mechanical properties that is related to the HC. Due to different ultrasonic wavespeeds of acoustic waves propagating along NN and SGS, alternating constructive and destructive interference signal can be detected by the transducer in a vertical scan. By analyzing the alternating period in a vertical scan, the phase velocity of guided waves (G) can be determined. An elaborated Fourier-based signal processing scheme [19] can be used to analyze the periodical phenomenon and extract the dispersion spectra of guided waves.

4. Equipment configuration and measurement method

Fig. 4 shows an equipment configuration of the AM used in the current research. The measurement system consists of a PVDF/LFB transducer, an ultrasound pulser/receiver, a digital oscilloscope, a translation stage with motion controller, and a computer. The pulser/receiver generates and detects ultrasonic waves through the transducer. The PVDF/LFB transducer has a large numerical aperture and a broadband frequency response. Large numerical aperture enables the LFB transducer to generate and detect guided waves propagating at low phase velocities. The frequency response of the transducer is shown in Fig. 5, in that a central frequency of slightly less than 4 MHz is observed. The output signal from the pulser/receiver is digitized by the oscilloscope and transmitted to the computer for signal processing. The translation stage controlled by the computer through the motion controller moves the transducer for a vertical scan. A coordinate system defined in Fig. 4 is used to explain the alignment of the transducer and claddings. The arc of the PVDF film of the transducer is coincident with the xz-plane. The cladding is aligned with its axial direction parallel with the x-axis. With this alignment, guided waves (G) can be generated by the LFB transducer, and propagates along the axial direction of the claddings.

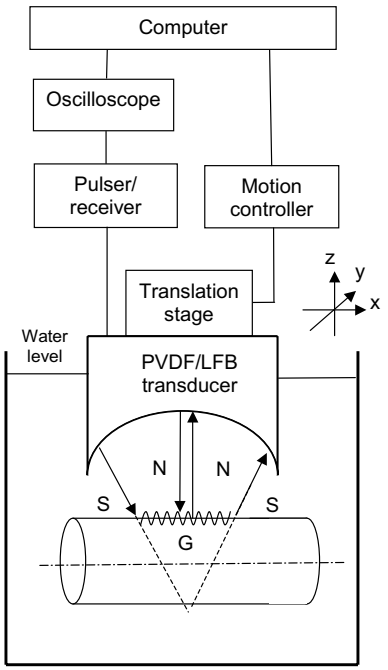

Fig. 4. A schematic showing the experimental configuration for the AM used for the characterization of HC in Zircaloy claddings.

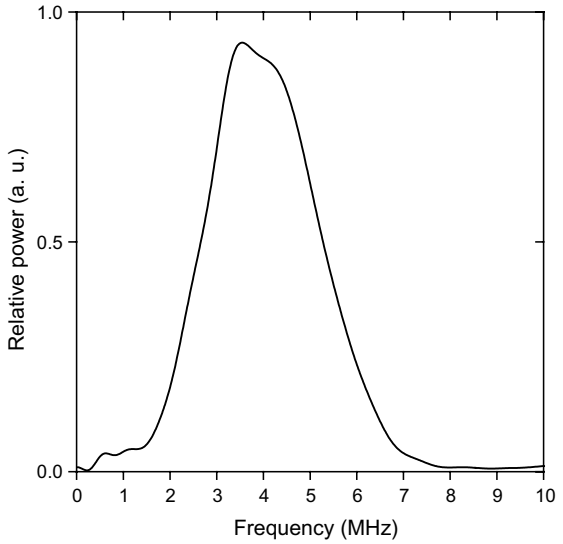

Fig. 5. A plot showing the frequency response of the PVDF/LFB transducer.

Fig. 6 shows a waveform measured with the AM for the archive cladding. In this figure, the horizontal axis denotes the elapsed time triggered at the arriving of the directly reflected signal (NN). The vertical axis denotes the relative amplitude of the detected acoustic signal. Fig. 6 contains multiple modes of guided waves.

Dispersive phase velocities of the guided waves are measured with the AM by a vertical scan of the LFB

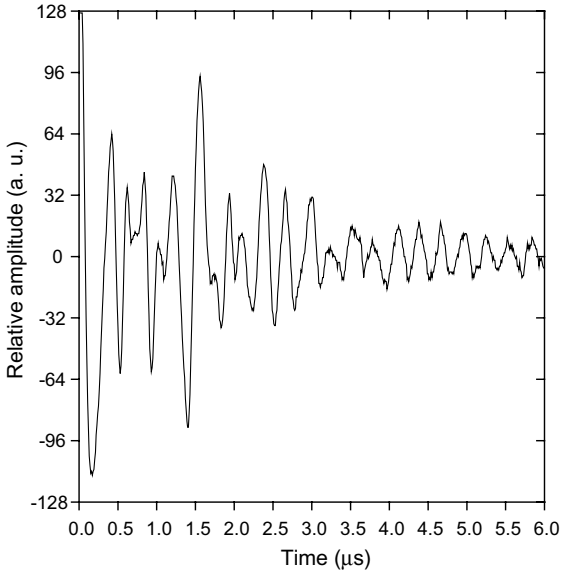

Fig. 6. A plot showing a waveform of guided waves for the archive Zircaloy cladding measured with the AM.

transducer, followed by a two-step signal processing scheme. The transducer is initially placed just above the sample, and then scanned away vertically from the sample. A total scanning distance of 5 mm with 200 steps is used to obtain a set of dispersion spectra. Waveform like that shown in Fig. 6 is collected at each step. A set of z-scan data for the archived sample is shown in a gray scale format in Fig. 7. In this figure, the horizontal axis denotes the elapsed time, the vertical axis denotes the z-position, and the gray scale represents the relative amplitude of acoustic waves.

Multi-mode dispersion spectra are further extracted from the z-scan data by a two-step signal processing scheme. The first step of the signal processing employs a two-dimensional fast Fourier transform (2D-FFT). In the 2D-FFT, the first FFT is taken with respect to time, and the second FFT with respect to the z-position. The 2D-FFT transforms the z-scan data into acoustic amplitude as a function of frequency (f) and wavenumber in z (k_z). A peak-detection routine is used to finds the trajectories with peak amplitudes in the f–k_z space. The dispersive phase velocity (V) of the guided wave is finally determined following Ref. [17] with the equation

$$V = V_0 \left(1 - \left(1 - \frac{k_z}{2f}\right)^2\right)^{-1/2}. \quad (1)$$

Here V_0 is the wavespeed in water, and (f, k_z) are data points in the trajectories of peak acoustic amplitude.

5. Results and discussions

Fig. 8 shows the measured dispersion spectra for the archive Zircaloy cladding sample using the quantitative AM technique. Two guided acoustic modes, labeled as A_0 and S_0, are observed. The A_0 mode is known as the fundamental anti-symmetric Lamb mode, and the S_0 mode is the fundamental symmetric Lamb mode [20]. In this research, the phase velocity of A_0 mode is used for a correlation with HC in the claddings. The A_0 mode shows a positive dispersion behavior, meaning that the phase velocity increases monotonically as the frequency increases.

The dispersion spectra of A_0 modes for the five cladding samples are plotted in Fig. 9. In a zoomed scale, the phase velocity of A_0 mode shows a decreasing trend due to the increase of HC. The trend of decreasing phase velocity in the A_0 mode can be supported by a physical foundation. When the the Zircaloy is filled with hydrogen molecules, they are similar to micro-voids and reduce the stiffness, and the phase velocity as well. It is also shown that the measurement in the dispersive phase velocity has a high resolution of better than 0.01 km/s, or 10 m/s with this AM technique.

A specific quantitative correlation between phase velocity and HC of claddings can be established by selecting an operation frequency. The operation frequency can be arbitrarily selected within the frequency range of A_0 mode. Currently, an operation frequency of 1.6 MHz is selected. Fig. 10 shows the phase velocity at the operation frequency of 1.6 MHz as a function of HC. The horizontal axis denoted by hydrogen

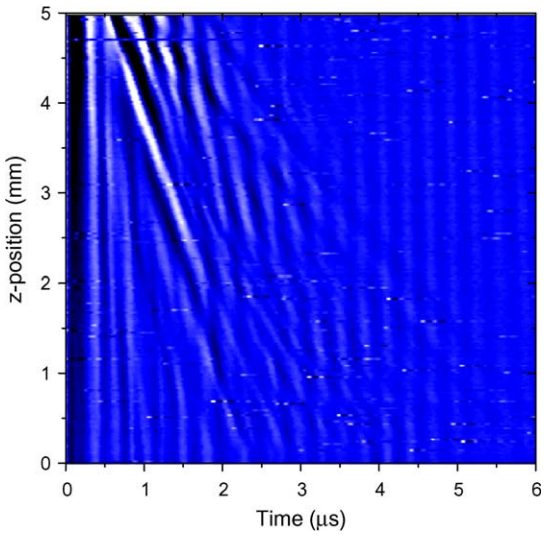

Fig. 7. A plot showing a z-scan data presented in a gray scale format for the archive Zircaloy cladding measured with the AM.

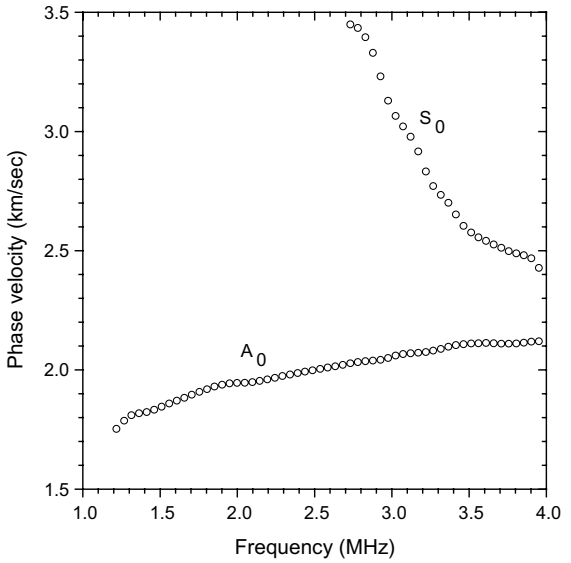

Fig. 8. A plot showing the measured dispersion spectra for the archive Zircaloy cladding measured with the AM.

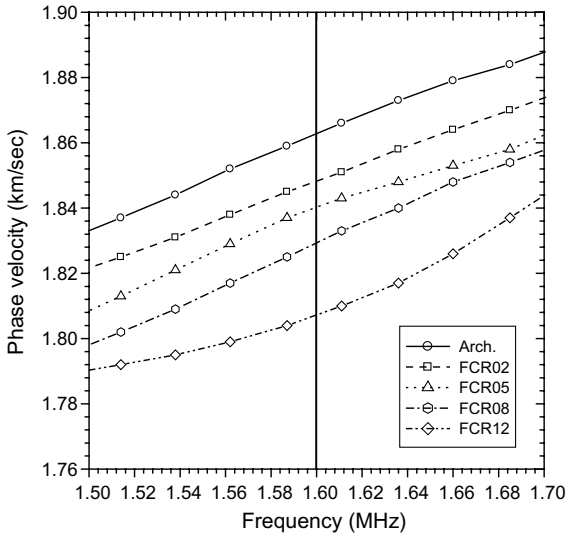

Fig. 9. A plot showing the measured A_0 modes for the five Zircaloy claddings with different HCs.

concentration is the average of measured HCs listed in Table 1. It is shown that the A_0 phase velocity at 1.6 MHz decreases almost linearly as the HC increases. With a linear regression, a negative slope of 5.022×10^{-5} km/s/ppm is obtained. In other words, a decrease in the phase velocity of 5.022 m/s at 1.6 MHz for the A_0 mode is associated with each 100 ppm of increase in HC for the current Zircaloy claddings. With the experimental data shown in Fig. 10, a better resolution of 100 ppm in measuring the HC is feasible with the quantitative AM technique.

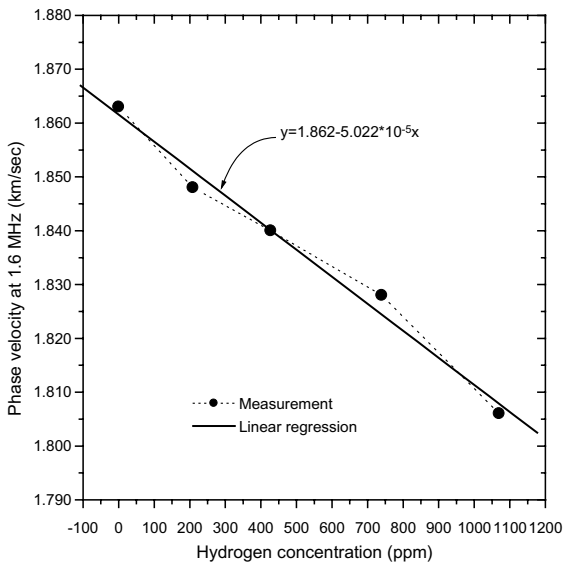

Fig. 10. A plot showing a correlation between the A_0 phase velocity at 1.6 MHz and HC in the Zircaloy claddings.

6. Conclusions

An ultrasonic NDE technique employing a low-frequency acoustic microscope (AM) is described for the characterization of HC in Zircaloy claddings with a satisfactory sensitivity. Very minor change in the phase velocity of the A_0 guided mode is successfully resolved and found to be decreasing as HC increases. A quantitative correlation between phase velocity and HC in Zircaloy claddings is successfully established. A resolution of 200 ppm in the HC measurement is demonstrated, and a better resolution of 100 ppm is feasible. Characterization of non-homogeneous hydride distribution in Zircaloy claddings is under investigation. This NDE technique is developed with an aim to have a better resolution and to be potentially applied to poolside inspection as well.

Acknowledgments

Financial support from National Science Council, Taiwan, through grant No. NSC91-NU-7-182-003 is gratefully acknowledged. Also kindly discussions and efforts for specimen preparations and hydrogen measurements by Dr R.C. Kuo and Dr C.T. Yang of the Institute of Nuclear Research (INER), Taiwan, ROC are acknowledged.

References

[1] C.E. Coleman, D. Hardie, J. Less. Common Met. 2 (1966) 168.
[2] J.-H. Huang, S.-P. Huang, J. Nucl. Mater. 208 (1994) 166.
[3] B. Cox, J. Alloys Comp. 256 (1997) 244.
[4] B. Cox, J. Nucl. Mater. 264 (1999) 283.
[5] S. Yamanaka, K. Higuchi, M. Miyake, J. Alloys Comp. 231 (1995) 503.
[6] S.B. Wisner, R.B. Adamson, Nucl. Eng. Design 185 (1998) 33.
[7] J. Bai, C. Prioul, J. Pelchat, F. Barcelo, in: Proceedings of the of International Conference of ANS/ENS, Avignon, France, 21–24 April 1991, p. 223.
[8] M. Garde, ASTM STP 1023, ASTM, Philadelphia, PA, 1989, p. 548.
[9] M. Garde, G.P. Smith, R.C. Pirek, ASTM STP 1295, ASTM, Philadelphia, PA, 1996, p. 407.
[10] K. Choo, Y. Kim, J. Nucl. Mater. 297 (2001) 52.
[11] G.A. Bickel, L.W. Green, M.W.D. James, T.G. Lamarche, P.K. Leeson, H. Michel, J. Nucl. Mater. 306 (2002) 21.
[12] R. Yasuda, M. Matsubayashi, M. Nakata, K. Harada, J. Nucl. Mater. 302 (2002) 156.
[13] A. Lois, H. Mendonca, M. Ruch, in: Proceedings of the 15th World Conference on Nondestructive Testing, Roma, Italy, 2000.
[14] V. Roque, D. Baron, J. Bourgoin, J.M. Saurel, J. Nucl. Mater. 275 (1999) 305.

[15] D. Laux, B. Cros, G. Despaux, D. Baron, J. Nucl. Mater. 300 (2002) 192.
[16] J.L. Singh, K.P. Prasannan, H.N. Singh, K.C. Sahoo, D.S.C. Purushotham, in: Proceedings of the 7th European Conference on Non-Destructive Testing, 1998.
[17] J. Kushibiki, N. Chubachi, IEEE Trans. Sonics, Ultras. SU-32 (1985) 189.
[18] D. Xiang, N.N. Hsu, G.V. Blessing, Ultrasonics. 34 (1996) 641.
[19] C.H. Yang, Rev. Progr. Quant. Nondestruct. Evaluat. 17 (1997) 177.
[20] B.A. Auld, Acoustic Fields and Waves in Solids, Krieger, Malabar, FL, 1990.